RSC Advances

ROYAL SOCIETY OF CHEMISTRY

www.rsc.org/advances

Mechanistic Study of CO Formation from CO_2 Using a Mixed-Metal Oxide of Tin, Iron, and Aluminum

Jian-Ping Shen [a], Paul D. Mobley [a], Laura M. Douglas [a], Jonathan E. Peters [a], Marty Lail [a]*, Jason S. Norman [a], and Brian Turk [a]

Received (in XXX, XXX) Xth XXXXXXXXX 20XX, Accepted Xth XXXXXXXXX 20XX
DOI: 10.1039/b000000x

A mechanistic study has been performed to show that a reduced mixed metal oxide derived from tin, iron, and aluminum oxides can remove oxygen from carbon dioxide. Thermogravimetric analysis confirms that reduction of the mixed-metal oxide likely involves the reduction of $SnO_2$and Fe_2O_3 phases. The reduced mixed-metal oxide can remove oxygen from carbon dioxide and this is shown using isotopically labelled $C^{18}O_2$ and mass spectroscopy. The ^{18}O-labelled mixed-metal oxide can transfer the abstracted oxygen to a different carbonaceous compound, in this case carbon monoxide. Oxygen is readily exchanged in the mixed-metal oxide. Under both oxidizing and reducing conditions ^{18}O is exchanged with unlabelled O resulting in the observation of all isotopomers.

Cite this: DOI: 10.1039/c0xx00000x

www.rsc.org/xxxxxx

Full Paper

Introduction

The use of CO_2 as a chemical feedstock is an appealing strategy for curbing greenhouse gas emissions. Numerous technologies are currently being developed to remove CO_2 from fossil power plant exhaust gases. The products of these processes are environmentally benign exhaust gas streams and concentrated CO_2 gas streams. If the CO_2 gas stream can be used as a reactant in a process which yields a more energetic product, such as a fuel or value-added intermediate, then the original fossil-fuel carbon has been renewed to utility for another application.

The potential for the upgrading of carbon dioxide through industrial processes has been investigated over the course of the past one-hundred years.[1] Attractive energy applications have included production of methanol from CO_2 by methane reforming (Carnol process), methane production by hydrogenation of CO_2 (Sabatier reaction), and production of carbon monoxide and hydrogen by reforming CO_2 with methane.[2-4] In addition, carbon dioxide can be combined with carbon and transformed into carbon monoxide by the Reverse-Boudouard reaction.[5] This transformation is thermodynamically favoured beginning at ~700°C. Cattolica et al have recently applied the Reverse-Boudouard reaction to upgrading of producer gas.[6] Several researchers have explored mixed-metal oxides for the Reverse-Boudouard reaction in the past and have been reviewed by several authors.[1, 7-19] Among them, some have explored the oxidation and reduction of iron on elemental carbon supports and impregnated in coal using techniques such as thermogravimetric analysis, $^{13}CO_2$ pulsed reactions, and temperature programmed desorption.[11, 13, 20, 21] Alkali carbonates have also been found to catalyse char gasification by CO_2 and some researchers have studied binary alkali-iron and alkaline-earth-iron mixed metal oxide systems and shown them to catalyse the formation of CO from carbon dioxide and chars.[22-28] Recently mixed metal oxides with nickel, ceria, and zirconia have been explored for carbon dioxide utilization by reforming to synthesis gas and by methanation.[29-31] Nickel oxides have also been studied explicitly for the Reverse-Boudouard reaction over Al_2O_3, TiO_2, and SiO_2 supports.[32] To our knowledge, mixed metal oxides containing Group VIII metals and reducible oxides of *p*-block metals, specifically tin, have not been reported for the gasification of carbon with CO_2.

We have developed several mixed metal oxides of tin and iron which are proposed to catalyse the Reverse-Boudouard reaction for production of CO from carbon feed stocks such as pet coke and biomass char. However, until now, little work has been done to show conclusively that the mixed-metal oxide materials operate by a metal-mediated extraction of oxygen from carbon dioxide to the reduced mixed-metal oxide surface, followed by transfer of the proposed oxygen to an external carbon source. In this paper we investigate the removal of oxygen from CO_2 by a reduced tin-iron mixed-metal oxide and show that the oxygen comes from carbon dioxide and is transferred intermolecularly to other carbon sources as shown in Scheme 1. The reaction was studied using isotopically-labeled $C^{18}O_2$, thermogravimetric analysis, and mass spectroscopy.

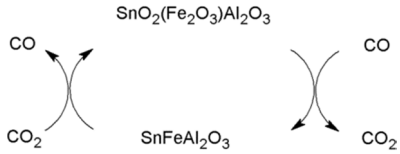

Scheme 1. Removal of oxygen from carbon dioxide by a reduced iron mixed-metal oxide.

Materials and Methods

Synthesis of $Fe_2O_3(SnO_2)_{1.41}(Al_2O_3)_{1.82}$ mixed-metal oxide

The mixed oxide was obtained by co-precipitation of metal salts from aqueous solutions using conventional procedures. Tin (IV) chloride, pentahydrate (Sigma Aldrich, 98%), iron (III) nitrate, nonahydrate (Sigma Aldrich, ≥98%), aluminum nitrate, nonahydrate (Sigma Aldrich, ≥98%) and ammonium hydroxide (BDH Aristar, 28-30%), were obtained and used as received without further purification.

For a 194.3g batch, 172.24 g (0.491 mole) $SnCl_4 \cdot 5H_2O$, 281.24 g (0.696 mole) $Fe(NO_3)_3 \cdot 9H_2O$, and 476.81g (1.271 mole) $Al(NO_3)_3 \cdot 9H_2O$ were dissolved into 1620g of deionized H_2O by mixing for at least 1 hour. This solution of metal salts, along with 504.07g (4.17 mole) of 28-30% NH_4OH were added to a precipitation tank containing 1500 g of DI water. The salt solution was added at a constant rate of 30 mL/min. The NH_4OH was added at a variable rate of 8-10 mL/min to maintain the pH of the precipitation at 8.0 ±0.2. The precipitation was stopped when all the metals salts were added to the precipitation tank and the pH was equal to 8.0. The precipitation was allowed to mix for an additional 45 minutes. The precipitate was filtered into two wet cakes and then washed with deionized (DI) water until the resulting filtrates contained chloride ion, as detected by a solution of 0.1M $Ag(NO_3)_2$, at a ppb level (based on K_{sp}). A loss on ignition (LOI) of each cake was used to determine the solid metal oxides content of each cake. By calculation, 195.3 grams solid were collected, yield 99%. Elemental analysis by ICP-MS showed Fe 18.7%, Sn 28.0%, Al 16.6%, theory Fe 20.3%, Sn 30.2%, Al 17.4%.

Thermo Gravimetric Analysis

Thermogravimetric analysis (TGA) was conducted using a TA Instruments TGA Q500 with Advantage for Q Series software. The plumbing of the TGA furnace was altered to receive gas for the sample purge from external mass flow controllers (MFCs), operated via an electronic control box. This allows for the

selection of additional gases for the sample purge compared to the standard Q500 design. Switching between gases was performed manually via in-line two-way valves, and flows were set according to MFC calibrations for each gas.

Two temperature programs were used involving multiple steps to demonstrate the addition and removal of oxygen from the surface of the mixed-metal oxide. For each analysis, a fresh sample (20-30 mg) was loaded in a tarred, platinum TGA pan at the start of the program. Each program extended over multiple days, and the same sample was used for the duration of the run. When necessary, the sample was held overnight or over-weekend in the closed TGA furnace under nitrogen at room temperature. In short, both programs describe heating the sample to 800°C and soaking for 60 minutes before cooling back down to 30°C using different gases to observe reducing, oxidizing, or purely thermal effects. In both programs, two cycles of the following steps are carried out. Thermal desorption in nitrogen is first observed followed by reduction with CO, then oxidation with CO_2.This series is repeated for the second cycle. In one program, the final oxidation with CO_2 is followed by oxidation with air, to observe any sites which may require a stronger oxidant than CO_2. In the second program, the second oxidation with CO_2 is followed by another reduction step, then oxidation with air, to confirm that the weight gain from the reduced sites oxidized in air is the same as the weight gain observed for oxidation of the reduced sites by carbon dioxide. Results are shown in Figure 2 and Figure 3 below.

AutoChem-MS Analysis with Isotopically –Labeled Gases

A Micromeritics' AutoChem II 2920 Chemisorption Analyzer was interfaced with a Dycor Quadrupole Mass Spectrometer was used to follow the transformations of carbon dioxide, carbon monoxide, and oxygen. The AutoChem II 2920 is a fully automated instrument capable of conducting precise chemical adsorption and temperature programmed reaction studies. The sample is contained in a quartz reactor housed in a clamshell furnace, programmable up to 1100 °C. Four gas inlets are equipped with high-precision, independently calibrated mass flow controllers to provide accurate delivery analysis gases. For these experiments, the Autochem was operated with constant flow of analysis gas through the sample reactor. Gases employed were ultra-high purity helium, a certified mixture of 20% CO in helium, and ^{18}O labelled CO_2. The isotopically labelled gases were purchased from Sigma-Aldrich and used as received. Experimental conditions for an exemplary experiment are given in Table 1 above. The results are given in Results and Discussion Section below.

Table 1: Exemplary parameters for $SnO_2Al_2O_3(Fe_2O_3)_3$ testing for $^{12}C^{18}O_2$ oxygen abstraction .

Step	Temp 1 (°C)	Temp 2 (°C)	Temp Ramp Rate (°C/min)	Gas	Flow (mL/ min)	Hold Time (min)
1	40	40	0	He	15	5
2	40	40	0	CO/He	15	5
3	40	800	10	CO/He	15	25
4	800	40	50	CO/He	15	0
5	40	40	0	N_2	15	5
6	40	40	0	$^{12}C^{18}O_2$	15	5
7	40	800	10	$^{12}CO_2$	15	25
8	800	40	50	$^{12}CO_2$	15	0
9	40	40	0	He	15	5
10	40	800	10	He	15	25
11	800	40	50	He	15	0
12	40	40	0	CO/He	15	5
13	40	800	10	CO/He	15	25
14	800	40	50	CO/He	15	0

Results and Discussion

Thermogravimetric Analysis

Mixed metal oxides containing tin are composed of tin-oxide phases which are known to have temperature-induced oxygen mobility.[33, 34] In considering the $SnO_2Fe_2O_3Al_2O_3$ mixed-metal oxide formulation and the given reaction conditions, it is sensible to question what types of oxygen containing sites are involved in the reduction of carbon dioxide and to consider the extent of oxygen transfer synergies. Reductions of both iron and tin have been reported over the range of temperatures examined in this study.[35-40] One simplistic perspective is to consider the oxygen in the mixed-metal oxide associated with SnO_2 as distinct from the oxygen which is associated with Al_2O_3 and likewise for the oxygen associated with Fe_2O_3. The nominal formulation of the mixed-metal oxide investigated here is $(Fe_2O_3)(SnO_2)_{1.41}(Al_2O_3)_{1.82}$ and is given in Figure 1 along with a oxygen in the mixed-metal oxide. The theoretical limit to the proposed mechanism which broadly describes a pathway for

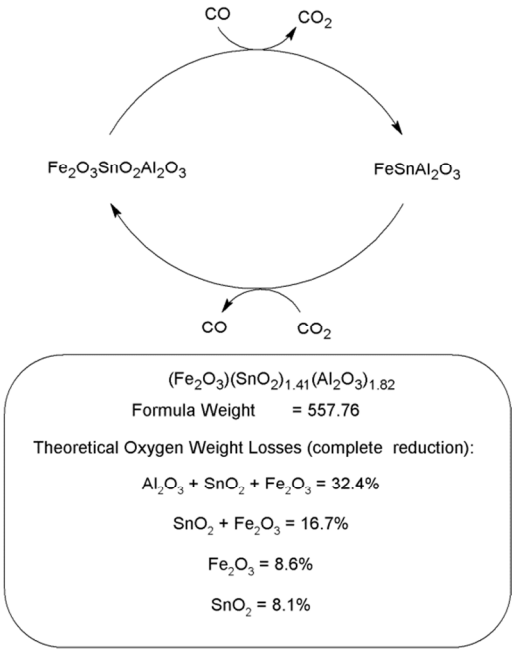

Figure 1: Oxidation and reduction scheme in thermo gravimetric experiments and nominal mixed-metal oxide formulation.

oxygen transfer. This mechanistic hypothesis can be tested by TGA. For example, the weight loss observed for loss of oxygen from SnO_2 alone (8.1% theoretical maximum) will be much

lower than a weight loss observed for all oxygen in the mixed-metal oxide. The theoretical limit to the weight loss due to complete oxygen loss is 32.4%. Intermediate weight losses could correspond to loss of oxygen from a combination of SnO_2 and Fe_2O_3 (16.7%), or only Fe_2O_3 (8.6%), or even by incomplete reduction of Fe_2O_3 to FeO (5.7%).

The data shown in Figure 2 and Figure 3 below immediately eliminate two hypotheses. Since the total weight loss is only approximately 21.6%, it is not possible that all the oxygen in the materials is available to reduction. Similarly, since an overall weight loss of 21.6% is observed starting from ambient, it is not likely that the oxygen originates exclusively from SnO_2 or exclusively from Fe_2O_3.

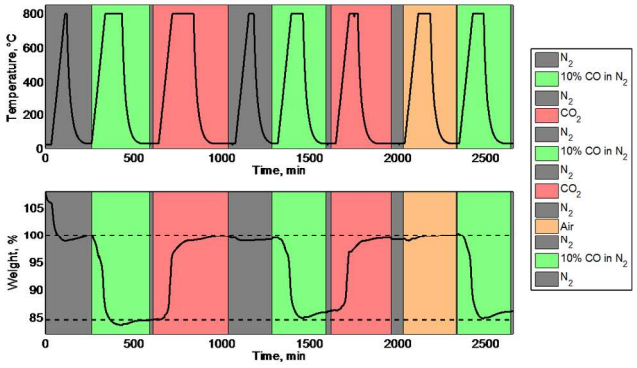

Figure 2: Percent weight change of mixed-metal oxide during thermo gravimetric analysis (bottom) and the corresponding temperature (top) in run 1.

Figure 2 shows that the weight loss observed when the material is heated from ambient to 800°C under flowing inert is approximately 7.4% (grey, inert). Presumably, this corresponds to loss of surface adsorbed and absorbed species such as adventitious water, oxygen, or carbon dioxide. A small weight gain of approximately 1% is observed while the sample is cooling from 800°C to 30°C, presumably a buoyancy effect. Other changes in weight are described afterwards in this document relative to the equilibrium weight after the initial desorption as suggested by the horizontal dotted lines on the weight profile. Following the inert thermal ramp, the weight of the sample is further decreased when the material is heated to 800°C in the presence of 10% CO (N_2 balance, green). The weight loss due to reduction by CO is approximately 15.4%. Subsequent oxidation with CO_2 results in a weight gain of about 99.1% of the previous weight loss (pink). Following the treatment with CO_2 about 0.5% of the initial weight is lost by ramping to 800°C in nitrogen. When the mixed-metal oxide is again treated with CO in a second reduction step, a smaller weight loss (~13.3%) is observed compared to the first reduction step. This is consistent with the hypothesis that some mixed-metal oxide is lost to deactivation, either reversible, or irreversible. One reversible deactivation route is the forward Boudouard Reaction, where one equivalent carbon is deposited from the disproportionation of two equivalents of CO. A follow-up oxidation step leads to a weight gain equal in magnitude to the weight loss observed during the previous reduction. A slight weight gain is then observed when the oxidized mixed-metal oxide is further oxidized while heated to 800°C in air, returning the sample to approximately the same weight observed after the initial desorption. This is consistent with the regeneration of active sites which may have been degraded in the prior reduction and oxidation cycles. After air oxidation, reduction with CO shows a 14.0% weight loss.

Figure 3 is very similar to Figure 2 regarding the magnitude of weight change events. However, after two cycles, the oxidized mixed-metal oxide is again reduced with CO then oxidized with air. The material shows a return to the weight observed prior to all reduction steps and at the end of each oxidation step. The comparison of Figure 2 and Figure 3 shows that the mixed-metal oxide can remove oxygen from CO_2, a relatively poor oxidant, as effectively as it can from O_2, a relatively strong oxidant. This is

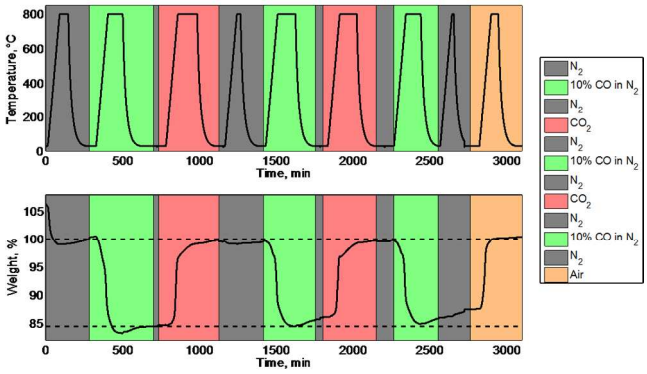

Figure 3: Percent weight change of mixed-metal oxide during thermo gravimetric analysis (below), and the corresponding temperature (above) in run 2.

manifest in the negligible weight gain which is observed when oxidation with air follows oxidation with CO_2 and by the negligible difference in weight gain between treating the reduced material with CO_2 or O_2 as oxidant.

The weight changes observed in the thermogravimetric analyses indicate that from ambient temperature to 800°C in the absence of a reductant, adventitious adsorbates (H_2O, CO_2, possibly O_2) are most likely desorbed from the surface of the mixed-metal oxide. While the initial weight loss here is in the same range as the weight loss expected from oxygen associated with SnO_2 (8.1% theoretical) and Fe_2O_3 (8.7% theoretical), the variation in the slightly lower observed losses (7.4% observed in Figure 2 and 6.0% observed in Figure 3*)*, along with mass spectroscopy data (discussed below, Figure 7) suggests that the weight loss is not due to O_2 but rather to CO_2. In the presence of a reductant, both SnO_2 and Fe_2O_3 sites are reduced when heated to 800°C, but Al_2O_3 sites do not appear to be reduced. The observed weight loss (15.5%), agrees well with the amount of oxygen calculated to be associated with SnO_2 and Fe_2O_3 (16.8%). The average overall observed weight loss from ambient (21.6%, Figure 2 and 20.6%, Figure 3*)* does not match as closely with combinations of theoretical predictions of complete oxygen removal from the various species; however it is not possible to calculate the total weight loss due to oxygen from ambient given the ambiguity of the adsorbed species. It is likely that the weight loss is due first to adventitious adsorbates, then to full reduction of SnO_2 and Fe_2O_3.It must be noted that the thermogravimetric analysis cannot be used to conclusively rule out coincidental

weight changes resulting from combinations of partial oxygen losses from SnO_2, Fe_2O_3, and Al_2O_3 sites. That is, the weight losses observed are still within the theoretical maxima for losing O_2 from the metal oxides. However, Figure 4 and Figure 5 show plots of the observed weight changes with temperature corresponding to Figure 2 and Figure 3, respectively. The data is displayed by purge gas over the temperature range from 0-800°C, thus for most weight changes observed when ramping to 800°C there is a corresponding static weight observation for cooling from 800°C. Each weight change trace is numbered to indicate that it is associated with a different step in the TGA program. The derivative plots indicate that changes in weight are likely due to three events and involve two types of active sites. The weight change observed during the initial temperature ramp in nitrogen (black) peaks distinctly at 100°C in agreement with the hypothesis that the initial weight loss involves the loss of adventitious absorbates. When the reduced mixed-metal oxide is oxidized by treatment with CO_2 (red traces), two separate events are observed to occur, the first at approximately 650°C and the second occurring at approximately 720°C. The bimodal distribution for weight change under oxidizing conditions is reproducible in both CO_2 treatment steps. These observations are consistent with oxygen abstraction from CO_2 occurring at two different sites, one active at slightly lower temperature than the other. In the reduction steps (green), a bimodal distribution is also observed. A low temperature weight change is observed at approximately 400°C and is minor compared to the higher temperature weight change observed at 700°C. A third minor weight change is also observable above 700°C but is not as pronounced as the primary peak. It is also observed that in the initial reduction cycle, weight changes are observed at slightly lower temperatures compared to the next two cycles. Future spectroscopic studies could be conducted to enhance the current understanding of this aspect of the mechanism.

Finally, in Figure 4, the sample is treated with air (orange) after the mixed-metal oxide has been oxidized with CO_2, and the rate of weight change during this event is small. However, Figure 5 shows treatment of the reduced sample with air. The mixed-metal oxide begins to gain weight at temperatures as low as 100°C, then demonstrates a marked increase in weight

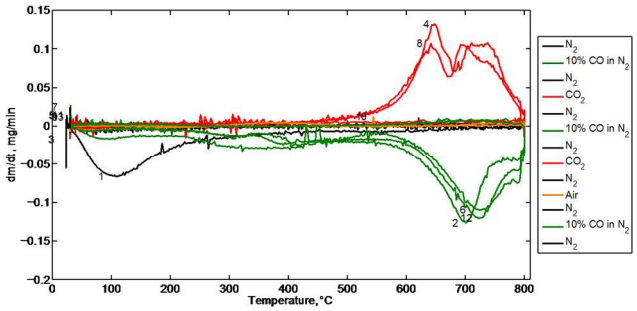

Figure 4: Rate of weight change of mixed-metal oxide versus temperature in run 1. The numbers denote the order of each step in the method to the left of its extreme.

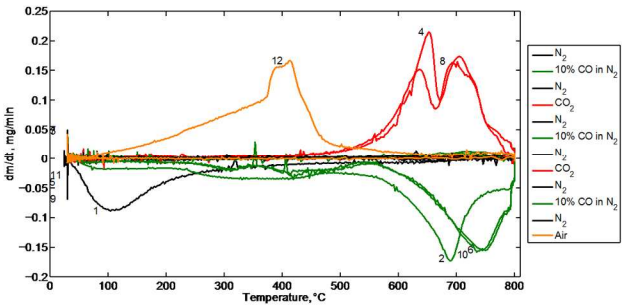

Figure 5: Rate of weight change of mixed-metal oxide versus temperature in run 2. The numbers denote the order of each step in the method to the left of its extreme.

change at approximately 375°C, with an additional peak at approximately 425°C. The observations of different peaks in the weight change plot support the hypothesis that there is more than one type of active site. This also shows the relative strengths of O_2 and CO_2 as oxidants and affinity of the mixed-metal oxide for O_2 relative to CO_2. Mixed-metal oxide oxidation by O_2 occurs at lower temperatures (~100-400°C) compared to CO_2 (~650-750°C).

AutoChem studies with Isotopically labelled $C^{18}O_2$

Mass spectroscopy (MS) experiments were conducted with isotopically labelled $C^{18}O_2$. The study reveals details about both the fate of the oxygen abstracted from CO_2 as well as the capability of the mixed-metal oxide to transfer metal-oxide-associated oxygen to external carbon sources. Details of the experiment are provided in the experimental section above. In short, the AutoChem is an atmospheric, fixed bed reactor with a quartz u-tube sample holder and a high-temperature furnace. The tube is purged with reactive gases and heated according to a temperature program. Gas exiting the AutoChem is analysed by MS. Isotopically-labelled $C^{18}O_2$, was used which contains heavy oxygen that is distinguishable by MS. The ^{18}O isotope is a stable isotope of oxygen with a low natural abundance and is useful to show the original molecular connectivity and its associations after undergoing chemical changes. In this study we used 97% $C^{18}O_2$ (balance $C^{16}O_2$) from Sigma-Aldrich. In contrast to the use of nitrogen and 10% CO in nitrogen during TGA experiments, ultra high purity helium and 20% CO in helium were used as purge gas and reducing gas for the mass spec studies, and as such the correlation between the two types of experiments is not exact.

In the presence of a mixed-metal oxide which abstracts oxygen from carbon dioxide, heavy oxygen (^{18}O) will be removed with the production of $C^{18}O$, which is two mass units heavier than $C^{16}O$. This is the primary product that we anticipated to observe by MS upon treatment of the reduced mixed-metal oxide with $C^{18}O_2$. It was postulated that this would oxidize the reduced mixed-metal oxide with ^{18}O, thus labelling the mixed-metal oxide. It was also anticipated that the labelled mixed-metal oxide could then be reduced again with CO with the resulting production of $C^{16}O^{18}O$, which would have a mass of 46 mass units, rather than 48 ($C^{18}O_2$) or 44 ($C^{16}O_2$). Figure 6 shows the mechanism envisioned to probe with the use of $C^{18}O_2$.

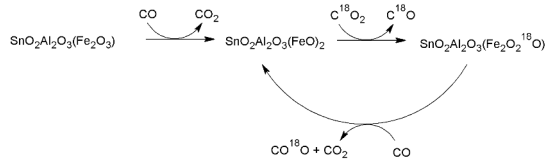

Figure 6: Oxidation and reduction scheme in the MS experiments.

An initial evaluation of the mixed-metal oxide was conducted by heating the mixed-metal oxide from ambient to 800°C under a purge of helium. Figure 7 shows the responses of the MS signals during analysis. The primary species detected under these conditions is CO_2, and data is consistent with desorption from two different sites. A small increase in the O_2 signal is observed as the sample nears 800°C. Water was not monitored in the analysis but is a likely an adsorbed species as well.

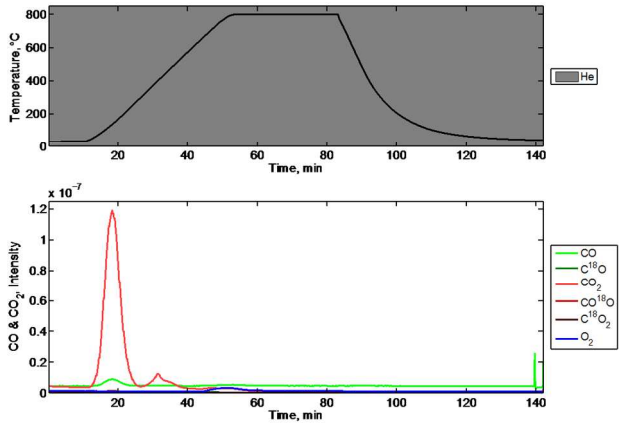

Figure 7: Mass spectrometry signals of relevant species over time (bottom) during an initial temperature ramp (top) in a helium purge.

Figure 8 shows the temperature dependence of the CO_2 desorption. The first desorption is observed between 50-250°C and shows a maximum intensity at approximately 150°C. Carbon monoxide is also detected to desorb during the initial inert temperature ramp. It is possible that this is indicative of the reaction mechanism. For instance, if some CO_2 is bound on the surface of the mixed-metal oxide, in the absence of a carbon source to reduce the mixed-metal oxide, CO_2 desorption from the mixed-metal oxide site is favoured over oxygen abstraction.

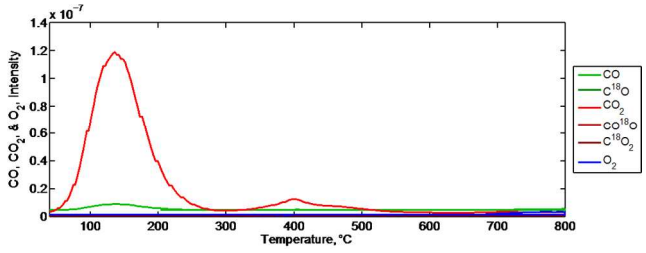

Figure 8: CO, CO_2, and O_2 intensity signals against temperature during an initial temperature ramp in a helium purge.

A four step experiment is shown in Figure 9. The mass spec signals are plotted with respect to time and are shown in the bottom plot. The corresponding temperature program used during evaluation is shown in the top plot. In the first step, shown in detail in Figure 10, the mixed-metal oxide was reduced by heating to 800°C in flowing 20% CO (balance He) with twenty-five minute soak time at 800°C. The intensities of the signals observed by MS are consistent in magnitude for the species we anticipated to observe in this step. CO is introduced as the reduction gas and we observe decreases in its peak intensity during the temperature ramp. Corresponding responses for CO_2 are observed and correlate strongly to the decrease in the CO signal. Unanticipated changes in the signals for other species are not observed during this stage. Figure 11 shows the temperature dependent behavior of the mass signals observed in step 1. Oxidation of the first type of site occurs at approximately 310°C while the latter oxidation begins just before 600°C.

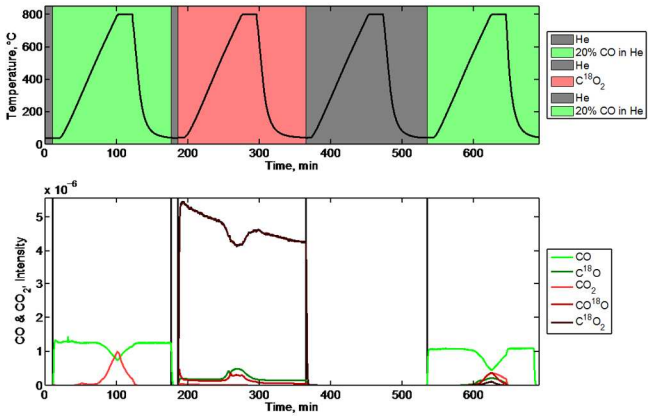

Figure 9: Mass spectrometry signals of relevant species over time (below), and the corresponding temperature (above).

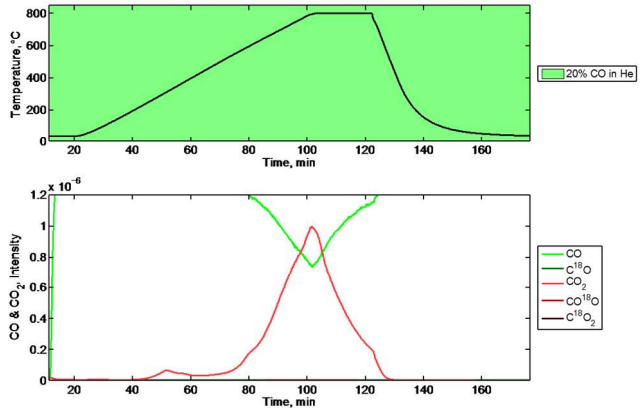

Figure 10: Mass spectrometry signals of relevant species during step 1 (below) and the corresponding temperature (above).

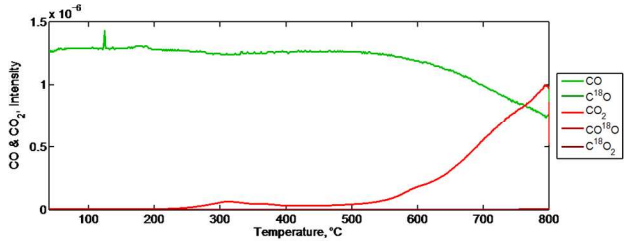

Figure 11: CO and CO_2 intensities versus temperature during step 1.

After cooling back down to 40°C, the reactor was purged with helium and the feed was switched to $C^{18}O_2$ for step 2, shown in detail in Figure 12. The mixed-metal oxide was then again heated

to 800°C, soaked for twenty-five minutes, and cooled to 40°C. In this step we anticipated formation of $C^{18}O$ (mass 30) as a result of the oxygen abstraction by the reduced material. While this was observed in correlation with a decrease in the signal for $C^{18}O_2$, and is consistent with abstraction of ^{18}O from labeled $C^{18}O_2$, we also observed a correlated increase in $C^{16}O^{18}O$. This observation is consistent with extraction of oxygen from labeled $C^{18}O_2$ to make $C^{18}O$, followed by reformation of carbon dioxide using unlabeled oxygen from the mixed-metal oxide to form $C^{16}O^{18}O$. Judging by the magnitude and correlation of the two signals, oxygen abstraction from CO_2 and oxygen abstraction from the mixed-metal oxide by CO occur at about the same rate under these experimental conditions. The temperature dependence of step 2 is shown in Figure 13 and appears to be unimodal and occurring at approximately 630°C for CO appearance and 650°C for $CO^{18}O$ appearance.

In step 3, displayed in Figure 14, the gas was switched to helium and the sample temperature was ramped, soaked and again cooled. This did not result in a change in any of the observed masses (28, 30, 32, 44, 46, and 48). In comparison, Figure 15 shows an initial desorption of the mixed-metal oxide when taken from ambient to 800°C in a helium purge. While a transition from Fe_2O_3 to Fe_3O_4 would be expected to produce a small amount of O_2, there is no increase in the signal for mass $32(O_2)$. In addition, when coupled to the initial weight loss observed in the thermogravimetric data, the lack of increase in the signal for $32(O_2)$ and observed increase in $44(CO_2)$ can best be explained as loss of surface adsorbed species (H_2O, CO_2) and strongly absorbed species (150°C, 400°C) without loss of oxygen postulated to come from SnO_2 in the absence of any reductant. The data shown in Figure 17 indicates that little detectable oxygen is liberated from the mixed-metal oxide by thermal reduction only, and that a reductant is required to achieve substantial oxygen depletion.

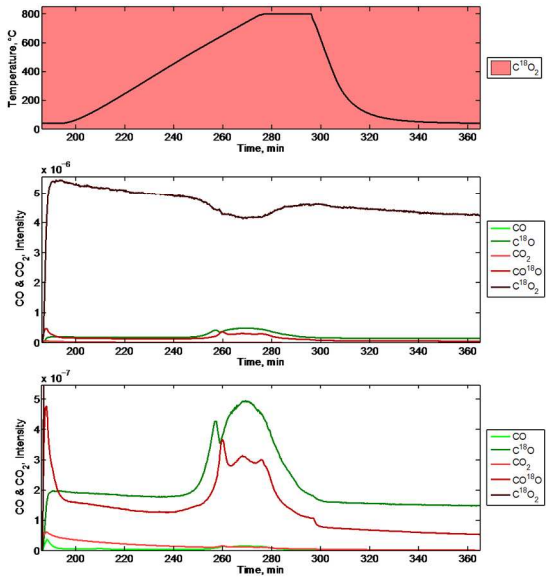

Figure 12: All mass spectrometry signals of relevant species during step 2 (middle), smaller intensity signals (bottom), and the corresponding temperature (top).

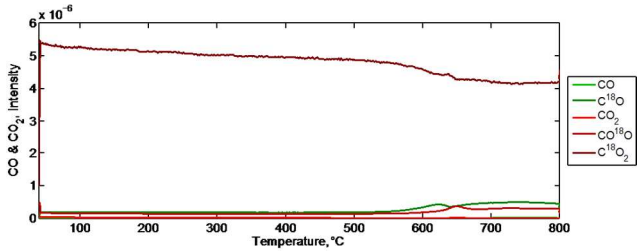

Figure 13: CO and CO_2 intensities versus temperature during step 2.

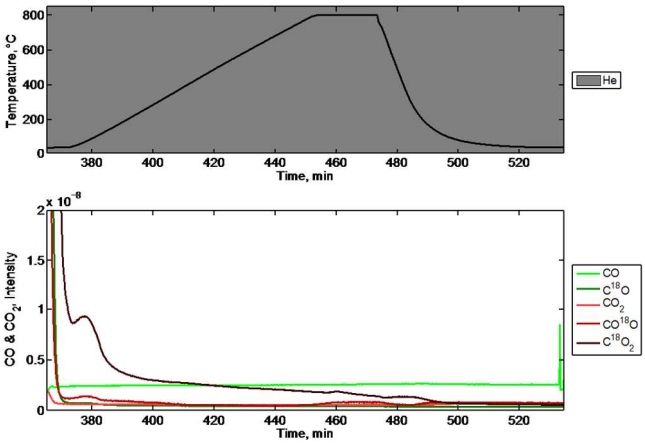

Figure 14: Mass spectrometry signals of relevant species during step 3 (below) and the corresponding temperature (above).

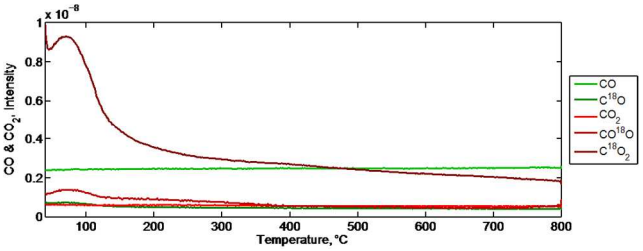

Figure 15: CO and CO_2 intensities versus temperature during step 3.

However, we also observed the formation of other species which can be explained in support of the proposed mechanism. Beginning with the smallest, $C^{18}O$ was observed to increase with decrease in CO at approximately 650°C. Two mechanisms can bepostulated for this observation. First, it is possible that carbon monoxide undergoes disproportionation to carbon and carbon dioxide and the carbon is deposited on the mixed-metal oxide surface where it picks up an ^{18}O from the labelled mixed-metal oxide. The second mechanistic route could be that carbon monoxide is absorbed on the surface of the mixed-metal oxide, is deoxygenated, and then re-oxygenated with a labelled ^{18}O. Further mechanistic studies, namely with isotopically-labeled ^{13}CO, could be conducted to discern this detail. In addition, both $CO^{18}O$ and $C^{18}O$ are observed to increase under reduction with CO. The detection of $CO^{18}O$ under these conditions supports the hypothesis that heavy oxygen (^{18}O) is abstracted from $C^{18}O_2$ by the mixed-metal oxide, and then added to a different carbon source, in this case carbon monoxide (CO), to produce partially labelled carbon dioxide ($CO^{18}O$). CO_2 was also observed to

increase with a strong correlation to the CO decrease. This increase is observed at a higher temperature (~800°C) compared to the appearances of $C^{18}O$ and $CO^{18}O$. CO_2 is observed presumably due to incomplete labelling of the mixed-metal oxide in the prior oxidation step. However, it could be postulated that the origin of 44 involves carbon deposition on the mixed-metal oxide under reducing conditions followed by CO_2 formation using unlabelled oxygen. An experiment with $^{13}CO_2$ could also be conducted to answer this question. Lastly, $C^{18}O_2$ is observed to increase in correlation with the decrease in CO. The increase in the signal intensity for $C^{18}O_2$ can only be accounted for by mechanistic routes which involve labelling of the mixed-metal oxide with ^{18}O in the previous oxidation step followed by transfer of the labelled oxygen during the subsequent reduction step. Transfer occurs either to a carbon which is absorbed by the mixed-metal oxide as CO before undergoing oxygen metathesis and oxygen addition, or to a carbon which is deposited on the mixed-metal oxide as elemental carbon before undergoing two oxygen additions with labelled ^{18}O which must have come originally from the labeled $C^{18}O_2$.

The AutoChem-MS studies using isotopically labeled $C^{18}O_2$ yield strong evidence in support of the hypothesis that $Fe_2O_3(SnO_2)_{1.39}(Al_2O_3)_{1.78}$ removes oxygen from CO_2 and transfers it to other carbon sources. The appearance of $C^{18}O$ and $C^{16}O^{18}O$ during oxidation of the reduced mixed-metal oxide with $C^{18}O_2$ shows the capability of the mixed-metal oxide to abstract oxygen from carbon dioxide as well as the ability to transfer mixed-metal oxide-ligated oxygen to an external carbon source. The appearance of $C^{16}O^{18}O$, $C^{18}O$, and $C^{18}O_2$ during reduction of the ^{18}O labelled oxidized mixed-metal oxide shows the ability of the mixed-metal oxide to transfer ligated oxygen's to carbon sources. It is clear that in addition to the transformations which occur on the desired reaction pathway, numerous other transformations occur in side routes on the same time scale. We propose that the mixed-metal oxide precursor is activated by reduction with CO producing CO_2 and vacancies in the coordination sphere of the active site. The active sites are occupied by oxygen of CO_2 and CO is produced. Oxygen from CO_2 is combined with CO to make CO_2 again and regenerate coordinatively unsaturated reactive metal centres. The coordinatively unsaturated metal centres can also bind CO through the nucleophilic carbonyl carbon, and at this point a

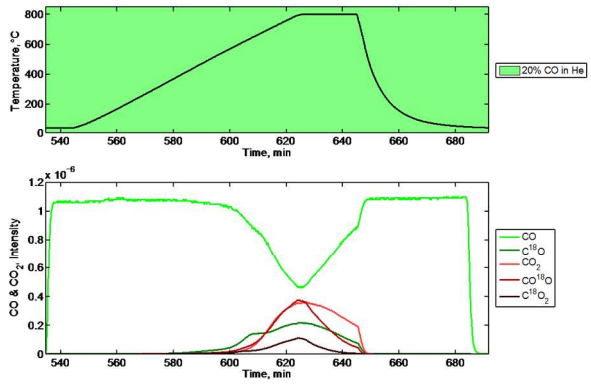

Figure 16: Mass spectrometry signals of relevant species during step 4 (below) and the corresponding temperature (above).

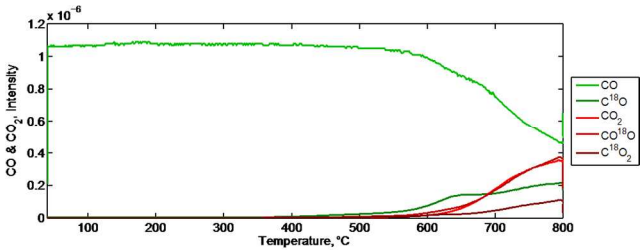

Figure 17: CO and CO_2 intensities versus temperature during step 4.

series of reversible insertions can be postulated to account for the observed oxygen scrambling.

Conclusions

In summary, the mechanistic investigation of the CO_2 utilization mixed-metal oxide $Fe_2O_3(SnO_2)_{1.39}(Al_2O_3)_{1.78}$ has been conducted using TGA and MS. The main findings are 1) thermogravimetric evidence suggests that oxygen from both Fe_2O_3 and SnO_2 are mobile and able to be removed from the mixed-metal oxide by reductants, 2) the reduced mixed-metal oxide is reactive towards CO_2 and removes oxygen from CO_2 to get back to its oxidized state, 3) mass spectroscopy experiments using isotopically-labeled carbon dioxide confirms that the reduced mixed-metal oxide abstracts oxygen from carbon dioxide, 4) the abstracted oxygen can be coupled to external carbon sources, and 5) side-reactions involving rapid exchange of oxygen by the mixed-metal oxide readily occur, resulting in overall high mobility of oxygen between the mixed-metal oxide, carbon dioxide, and carbon monoxide.

Notes and references

[a] *Energy Technology Division, RTI International, 3040 Cornwallis Rd., Research Triangle Park, North Carolina, USA. Fax: 09195418002; Tel: 09194855703; E-mail: mlail@rti.org*

† Electronic Supplementary Information (ESI) available: [details of any supplementary information available should be included here]. See DOI: 10.1039/b000000x/

‡ The authors would like to acknowledge Ernest W. Johnson, Kelly Amato, and Gary B. Howe of RTI International for providing analytical support for this work. The authors also acknowledge and thank the United States Department of Energy, National Energy Technology Laboratory, Office of Fossil Energy for funding this work under DOE Cooperative Agreement No. DE-FE0004329.

.

1. M. Halmann and M. Steinberg, *Greenhouse Gas Carbon Dioxide Mitigation Science and Technology*, Lewis Publishers, Washington, D.C., 1999.
2. M. Steinberg, Brookhaven National Lab, Upton, NY, December 1995.
3. S. K. Hoekman, A. Broch, C. Robbins and R. Purcell, *International Journal of Greenhouse Gas Control*, 2010, **4**, 44-50.
4. F. Fischer and H. Tropsch, *Brennst. Chem.*, 1928, **9**, 29-46.
5. K. Nagase, T. Shimodaira, M. Itoh and Y. Zhemg, *Physical Chemistry Chemical Physics*, 1999, **1**, 5659-5664.

6. C. K. Acharya, F. Jiang, C.-h. Liao, P. Fitzgerald, K. S. Vecchio and R. J. Cattolica, *Fuel Processing Technology*, 2013, **106**, 201-208.
7. S. Yokoyama, K. Miyahara, K. Tanaka, I. Takakuwa and J. Tashiro, *Fuel*, 1979, **58**, 510-513.
8. T. Suzuki, H. Ohme and Y. Watanabe, *Energy and Fuels*, 1994, **8**, 649-658.
9. F. Carrasco-Marin, J. Rivera-Utrilla, E. U. Hidalgo and C. Moreno-Castilla, *Fuel*, 1991, **70**, 13-16.
10. A. P. Dhupe, A. N. Gokarn and L. K. Doraiswamy, *Fuel*, 1991, **70**, 839-844.
11. H. Ohme and T. Suzuki, *Energy and Fuels*, 1996, **10**, 980-987.
12. F. Akiyama, *Chemistry Letters*, 1997, 643-644.
13. T. Kodama, S. Miura, T. Shimuzu, A. Aoki and Y. Kitayama, Abstr. 4th Int. Conf. on Carbon Dioxide Utilization, Kyoto, Japan, 1997.
14. R. T. Yang and C. Wong, *Journal of Catalysis*, 1983, **82**, 245-251.
15. K. J. Huttinger and O. W. Fritz, *Carbon*, 1991, **29**, 1113-1118.
16. H. Ono, M. Kawabe, H. Amani, M. Tsuji and Y. Tamaura, Abstracts of the Fourth International Conference on Carbon Dioxide Utilization, Kyoto, Japan, September, 1997, P-004.
17. M. Steinberg and Y. Dong, Abstracts of the International Conference on Carbon Dioxide Utilization, Bari, Italy, September 1993.
18. M. Steinberg, Abstracts of the Third International Conference on Carbon Dioxide Utilization, Norman, Oklahoma, May, 1995.
19. B. J. Wood and K. M. Sancier, *Catalysis Reviews-Science and Engineering*, 1984, **26**, 233.
20. T. Suzuki, K. Inoue and Y. Watanabe, *Energy and Fuels*, 1988, **2**, 673.
21. T. Suzuki, K. Inoue and Y. Watanabe, *Fuel*, 1989, **68**, 626.
22. J. M. Saber, J. L. Falconer and L. F. Brown, *Fuel*, 1986, 1356.
23. J. M. Saber, J. L. Falconer and L. F. Brown, *Journal of the Chemical Society, Chemical Communications*, 1987, 445.
24. S. R. Kelemen and H. Freund, *Carbon*, 1985, **23**, 723.
25. S. Yokoyama, K. Miyahara, K. Tanaka, J. Tashiro and I. Takakuwa, *Journal of the Chemical Society of Japan*, 1980, **6**, 974.
26. T. Suzuki, M. Mishima and Y. Watanabe, *Chemistry Letters*, 1982, **11**, 985.
27. J. Carrazza, W. T. Tyose, H. Heinemann and G. A. Somorjai, *Journal of Catalysis*, 1985, **96**, 234.
28. Y. Ohtsuka, K. Hosoda and Y. Nishiyama, *Journal of the Fuel Society of Japan*, 1987, **66**, 1031.
29. M. B. Gawande, R. K. Pandey and R. V. Jayaram, *Catalysis Science and Technology*, 2012, **2**, 1113-1125.
30. P. Kumar, Y. Sun and R. O. Idem, *Energy and Fuels*, 2008, **22**, 3575.
31. F. OCampo, B. Louis and A. Roger, *Applied Catalysis a-General*, 2009, **369**, 90.
32. T. Osaki and T. Mori, *Reaction Kinetics and Catalysis Letters*, 2006, **89**, 333-339.
33. J. Maier and W. Gopel, *Journal of Solid State Chemistry*, 1988, **72**, 293-302.
34. J. Mizusaki, H. Koinuma, J.-I. Shimoyama, M. Kawasaki and K. Fueki, *Journal of Solid State Chemistry*, 1990, **88**, 443-450.
35. X. Gao, J. Shen, Y. Hsia and Y. Chen, *Journal of the Chemical Society, Faraday Transactions* 1993, **89**, 1079-1084.
36. B. Hou, H. Zhang, H. Li and Q. Zhu, *Chinese Journal of Chemical Engineering*, 2012, **20**, 10-17.
37. B.-S. Kim, J.-c. Lee, H.-S. Yoon and S.-K. Kim, *Materials Transactions*, 2011, **52**, 1814-1817.
38. R. Padilla and H. Y. Sohn, *Metallurgical Transactions B*, 1979, **10B**, 1979-1109.
39. A. R. Mitchell and R. H. Parker, *Minerals Engineering*, 1988, **1**, 53-66.
40. R. Sasikala, N. M. Gupta and S. K. Kulshreshtha, *Catalysis Letters*, 2001, **71**, 69-73.